STM JOURNALS

Journal of
Polymer & Composites

ISSN: 2321-2810 (Online)
ISSN: 2321-8525 (Print)
Volume 13, Special Issue 3, 2025
DOI (Journal): 10.37591/JoPC

https://journals.stmjournals.com/jopc

Research JoPC

Role of Prey Refuge in Predator-Prey Dynamics with Nonlinear Functional Responses: A Mathematical Approach

Surabhi Pareek[1], Randhir Singh Baghel[2,*]

Abstract

The Beddington-DeAnglis and Holling type II functional response with prey refuge are used in this study to propose and assess a prey-predator system. This study looks at the ecological effects of prey refuge and how it affects predator-prey relationships, highlighting how functional responses influence population dynamics. The dynamical behavior of the model has been shown, which consist the existence of positivity, boundedness, local stability, and global stability. In addition, stability is derived using the Routh-Hurwitz criterion. The effect of the attack rate of generalist predators on specialist predators, the biological effect of the attack rate and the inhibitory effect are discussed. Hopf bifurcation is discussed with carrying capacity k_1*. Moreover, the Center Manifold theorem has been used to establish the stability of non-hyperbolic equilibrium sites. Simulations are carried out using MATLAB's ODE45 solver for numerical validation and to see the model's dynamic behavior. These findings validate the theoretical theory and provide examples of a range of dynamical situations, such as oscillatory behavior and stability transitions, which is a powerful approach to exploring the dynamic behavior of ecological models. Numerical findings are also provided to demonstrate our analysis. Lastly, conclusion has been given. With potential uses in conservation biology and resource management, the study adds to the body of literature on ecological modeling by offering a sophisticated method for examining intricate predator-prey relationships. Overall, by providing a sophisticated framework for comprehending intricate predator-prey dynamics, this study advances the field of ecological modeling. The results offer insights into how behavioral adaptations and ecological restrictions might impact predator-prey interactions, which may find use in conservation biology and resource management.*

Keywords: Prey-predator system, boundedness, stability, global stability, bifurcation, center manifold theorem

INTRODUCTION

In ecology, interactions between predators and prey occur at higher trophic levels and predators can affect prey populations directly and indirectly [1, 2]. Refuge shows an important part in prey predator model system. Also, if prey species are in large number, they have refuge ability by creating herds, it shows decreased predation of the prey [3-5]. By including prey refuge, one aims to account for a portion of the prey population that is inaccessible to predators, reducing the effective prey availability. This can influence the form and strength of the functional response[6,7]. In ecological research, understanding how prey species avoid predation is crucial. One significant strategy is the use of refuges, which are areas or conditions that provide safety from predators [27-29]. The predator's indirect influence involves the prey population, which has the potential to alter prey behavior, the predator's direct effect involves predating the prey [8-10].

*__Author for Correspondence__
Randhir Singh Baghel

[1]Research Scholar, Department of Mathematics, Poornima University, Jaipur, Rajasthan, India
[2]Associate Professor, Department of Mathematics, Poornima University, Jaipur, Rajasthan, India

Received Date: November 25, 2024
Accepted Date: February 08, 2025
Published Date: May 01, 2025

Citation: Surabhi Pareek, Randhir Singh Baghel. Role of Prey Refuge in Predator-Prey Dynamics with Nonlinear Functional Responses: A Mathematical Approach. Journal of Polymer & Composites. 2025; 13(Special Issue 3): S523–S537p.

Food chains in ecosystems where one prey interacts with multiple predators, leading to highly nonlinear interactions. This is indeed a complex system that requires models capable of handling these nonlinearities, especially through nonlinear functional responses. Functional responses like Holling type I-IV, Ivlev, Crowly-Martin, Beddinton-DeAngelis, etc. are major aspect of the ecological model system that are used in many biological studies [11-18]. By altering the predator's functional reaction to prey density, prey refuge can have a substantial impact on predator-prey dynamics in ecological modeling. In order to comprehend energy transfer between trophic levels, functional responses like Holling I, II, III and IV functional responses explain how the rate of predation (i.e., prey consumption per predator) varies with prey density. By lowering the effective prey density that predators encounter, prey refuge places or circumstances where animals are less susceptible to predation can change this dynamic [19-26].

The dynamics of a three-species food chain model which consists of prey, specialist predator, and generalist predator are the main focus of our research. The Routh-Hurwitz criterion, which establishes stability constraints based on the characteristic polynomial of the system, is used to determine local asymptotic stability. Lyapunov functions, which aid in proving stability across the whole phase space, are used to illustrate global asymptotic stability. After that, we have established Hopf bifurcation. In cases where the equilibrium points are non-hyperbolic meaning they have at least one eigenvalue with zero real part the system's stability cannot be determined solely by the sign of eigenvalues, as standard methods like the Routh-Hurwitz criterion are not applicable. This is where the Center Manifold Theorem becomes essential. Lastly, a few numerical simulations and graphical explanations are provided for each of the analytical results of this work. This is a more realistic and comprehensive approach, as it mirrors complex food web structures found in many ecosystems. In ecological research, understanding how prey species avoid predation is crucial. One significant strategy is the use of refuges, which are areas or conditions that provide safety from predators.

Motivation and Novelty

In our paper formulation of mathematical model based on three species food chain with prey refuge have been studied using Beddington DeAnglis and Holling type II functional responses. The Beddington-DeAnglis and Holling type II responses are especially helpful in modeling situations in which predators become more effective at increasing prey densities and less effective at lower densities. To improve the system's stability, the study combines these two functional responses together. This method can result in more resilient and stable ecosystem dynamics and enables a more sophisticated portrayal of predator-prey interactions. The attack rate of a generalist predator significantly influences the mathematical modeling of predator-prey dynamics. The attack rate directly determines the form and parameters of the functional response, which describes how the predator's consumption rate changes with prey density. Higher attack rate, increases the predator's efficiency in capturing prey, leading to a rapid decline in prey population. This can result in greater oscillations in population sizes and potentially destabilize the system if the prey population drops too low. Lower attack rate, decreases the predator's efficiency, allowing the prey population to grow, which might reduce oscillations and stabilize the system. Predator prey models demonstrate inhibitory effects in population dynamics, since the presence of predators slows the increase of prey populations. This interaction can keep the prey from growing too much and stabilize the populations. Also, the Center Manifold Theorem is a powerful tool in dynamical systems theory, particularly useful for analyzing the stability of non-hyperbolic equilibrium points. The Center Manifold theorem facilitates the analysis of a system's stability by lowering its dimensionality in the vicinity of a nonhyperbolic equilibrium point. Main objective is to examine the impact of functional responses on stability, assess the role of attack rate in predator-prey dynamics, explore the inhibitory effect of predators on prey growth, analyze stability and bifurcation behavior, introduce and assess prey refuge mechanism. This model is completely new as it integrates the Beddington-DeAngelis functional response and the Holling type II functional responses, which has not been previously combined in ecological research.

The article is given below: In part 2, model formulation of the non-spatial system has been given. In part 3, some definitions related to work are given. In part 4, dynamical behavior is analyzed. It is shown that equilibrium points exist then stability has been checked at each of the equilibrium points. Moreover, Global stability, effect of attack rate of generalist predator on specialist predator, bifurcation of the model, center manifold theorem have been performed. In part 5, numerical simulations have been given. Finally, in part 6, discussion and conclusion has been given.

SYSTEM MODEL FORMULATION

Now, we consider the prey-predator interaction model with impact of refuge. A schematic diagram is shown in Figure 1. Some ecological parameters are shown in Table 1. To propose the model system the assumptions are as below:

- Prey density is shown by u_1, specialist predator density is shown by u_2, and generalist predator density is shown by u_3.
- The prey species becomes larger with growth rate τ.
- k_1 shows carrying capacity.
- Prey and specialist predator succeed Holling type-II functional response.
- Specialist predator and generalist predator succeed Beddington functional response.

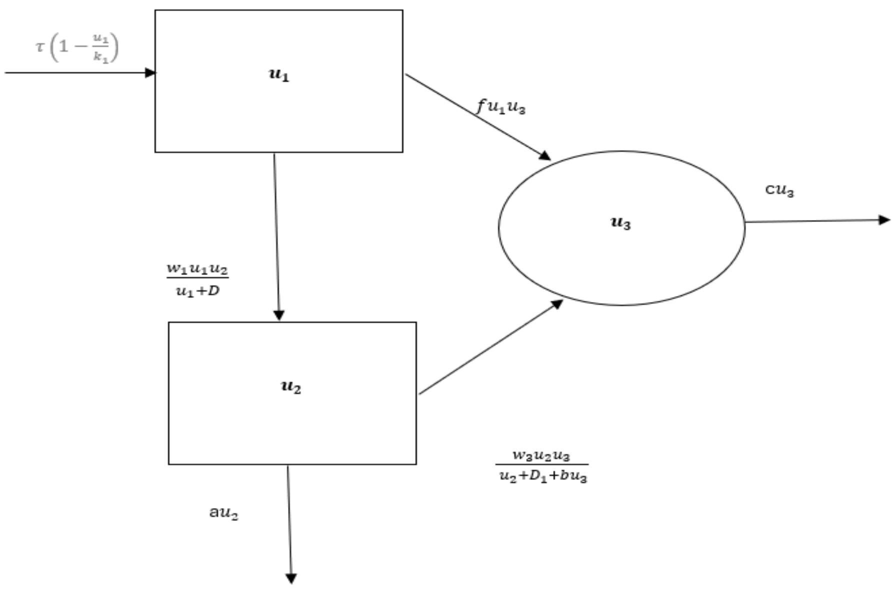

Figure 1. Schematic diagram of model system.

Table 1. Ecological Parameters.

Parameters	Meaning
τ	Growth rate of prey
k_1	Carrying capacity of prey
w	Attack rate of specialist predator on prey
w_1	Conversion rate of prey to specialist predator
$\boldsymbol{D}$	Half saturation constant of prey
$\boldsymbol{f}$	Attack rate of generalist predator on prey
$\boldsymbol{d}$	Conversion rate of prey to a generalist predator
$\boldsymbol{w_3}$	Conversion rate of specialist predator to a generalist predator
a	Natural death rate of specialist predator
c	Natural death rate of generalist predator
$\boldsymbol{D_1}$	Half saturation constant predator
b	Inhibitory effect

The model is expressed as below:

$$\frac{du_1}{dt} = \tau u_1\left(1-\frac{u_1}{k_1}\right) - \frac{wu_1u_2}{(u_1+D)} - fu_1u_3 \tag{1}$$

$$\frac{du_2}{dt} = \frac{w_1u_1u_2}{u_1+D} - au_2 - \frac{w_2u_2u_3}{u_2+D_1+bu_3} \tag{2}$$

$$\frac{du_3}{dt} = -\frac{w_3u_2u_3}{u_2+D_1+bu_3} - cu_3 + du_1u_3 \tag{3}$$

Subject to IC: $u_1(0) > 0, u_2(0) > 0, u_3(0) > 0$

DYNAMICAL BEHAVIOR

In this part, we will discuss positivity, boundedness, stability, and bifurcation of the system.

Positivity

The concept behind determining the positivity of the solutions is that since we are working with population dynamics systems, it is crucial to make sure that we don't get negative values. Populations in the system never go extinct because of the positives we discovered. For this purpose, we integrate the equations by using initial conditions, we get

$$u(t) = u(0)\left(\int_0^t \left[\tau\left(1-\frac{u_1}{k_1}\right) - \frac{wu_2}{(u_1+D)} - fu_3\right] ds\right)$$

Hence, if the initial conditions are non-negative then the right side is positive.

Boundedness

In this part, we prove the boundedness of the system. The term boundedness in population dynamics refers to the physiological stability of the system. It indicates the system is conducted in an appropriate manner. Theorem 1: Solutions of the model system (1)-(3) is uniformly bounded in R_+^3.

Proof: Let solution of the model (1)-(3) is$(u_1(t), u_2(t), u_3(t))$. Let us suppose a function $(u_1, u_2, u_3) = u_1 + u_2 + u_3$, then we have$\frac{d\psi}{dt} = \tau u_1\left(1-\frac{u_1}{k_1}\right) - \frac{u_1u_2}{(u_1+D)}(w-w_1) - u_1u_3(f-d) + \frac{u_2u_3}{u_2+D_1+bu_3}(w_2-w_3) - au_2 - cu_3$

Then we get $l > 0$, in a way that$\frac{d\psi}{dt} + \zeta\phi \le l$, which implies that: $\phi(t) \le \phi(0)e^{-\zeta t} + \frac{l}{\zeta}\left(1-e^{-\zeta t}\right) \le \max\left(\phi(0), \frac{l}{\zeta}\right)$. Hence, the theorem is proved.

Equilibrium Points and Stability

This analysis gives four equilibrium points (i) $E_1 = (0,0,0)$ (ii) $E_2 = (k_1, 0, 0)$ (iii) $E_3 = \left(\frac{c}{d}, 0, \frac{\tau}{f}\left(1-\frac{c}{dk_1}\right)\right)$ (iv) $E_4 = (\tilde{u}_1, \tilde{u}_2, \tilde{u}_3)$

Stability Analysis

In this part, first linearize the system to get the stability then find the Jacobian matrix.

Theorem 2: Eigen values of $J(E_1)$ is a saddle point. Proof: Here$E_1 = (0,0,0)$. Then, $J(E_1)$ is given:$J(E_1) = \begin{bmatrix} \tau & 0 & 0 \\ 0 & -a & 0 \\ 0 & 0 & -c \end{bmatrix}$

The eigenvalues of E_1 are $\tau, -a, -c$. Then, E_1 is a saddle point. *Theorem 3*: E_2 is LAS if $-a > \frac{wk_1}{k_1+D}$ and $-c > dk_1$.

Proof: $J(E_2)$ is as follows:

$$J(E_2) = \begin{bmatrix} -\tau & \frac{w}{k_1 + D} & -fk_1 \\ 0 & -a + \frac{wk_1}{k_1 + D} & 0 \\ 0 & 0 & -c + dk_1 \end{bmatrix}$$

The eigen values of E_2 are $-\tau, -a + \frac{wk_1}{k_1+D}$ and $-c + dk_1$. Therefore, E_2 is LAS if $-a > \frac{wk_1}{k_1+D}$ and $-c > dk_1$.

Theorem 4: $J(E_3)$ is LAS if $a > \frac{w_1 c}{c+dD} + \frac{w_2\tau(dk_1-c)}{fdk_1D_1+b\tau-cb\tau}$ and saddle point if $< \frac{w_1 c}{c+dD} + \frac{w_2\tau(dk_1-c)}{fdk_1D_1+b\tau-cb\tau}$.

Proof: $E_3 = \left(\frac{c}{d}, 0, \frac{\tau}{f}\left(1 - \frac{c}{dk_1}\right)\right)$, exists. $J(E_3)$ is as follows:

$$J(E_3) = \begin{bmatrix} \frac{-cw}{k_1 + D} & \frac{wc}{c + dD} & \frac{fc}{d} \\ & & 0 \\ & & \frac{d\tau}{f}\left(1 - a + \frac{w_1 c}{c + dD}\right. \\ \left.\frac{c}{dk_1}\right) & \frac{w_2\tau(dk_1 - c)}{fdk_1D1 + b\tau - cct} & 0 \\ \frac{w_3\tau(dk_1 - c)}{fdk_1D_1 + b\tau - cb\tau} & & 0 \end{bmatrix}$$

Thus, the characteristic roots $J(E_3)$ is as given: $-a + \frac{w_1 c}{c+dD} + \frac{w_2\tau(dk_1-c)}{fdk_1D_1+b\tau-cb\tau}, \frac{-\tau c}{k_1 d}, 0$
Hence, $J(E_3)$ is LAS if $a > \frac{w_1 c}{c+dD} + \frac{w_2\tau(dk_1-c)}{fdk_1D_1+b\tau-cb\tau}$ and saddle point if $a < \frac{w_1 c}{c+dD} + \frac{w_2\tau(dk_1-c)}{fdk_1D_1+b\tau-cb\tau}$

Theorem 5: E_4 is LAS, if conditions satisfy (i) A, B and $C > 0$, (ii) $AB > C$.
Proof: Now, for the equilibrium point $E_4 = (\tilde{u_1}, \tilde{u_2}, \tilde{u_3})$, exists. Thus $J(E_4)$ is as following:

$$J(E_4) = \begin{bmatrix} y_{11} & y_{12} & y_{13} \\ y_{21} & y_{22} & y_{23} \\ y_{31} & y_{32} & y_{33} \end{bmatrix}$$

where, $y_{11} = \tau - \frac{wu_2}{u_1+D} + \frac{wu_1u_2}{(u_1+D)^2}, y_{12} = \frac{wu_1}{(u_1+D)}$, $y_{13} = -fu_1, y_{21} = \frac{wu_2}{u_1+D} - \frac{w_1u_1u_2}{(u_1+D)^2}$,
$y_{22} = -a + \frac{wu_1}{u_1+D} - \frac{w_2u_2u_3}{(u_2+D_1+bu_3)^2} + \frac{w_2u_3}{(u_2+D_1+bu_3)}$,
$y_{23} = \frac{w_2u_2}{(u_2+D_1+bu_3)} - \frac{bw_2u_2u_3}{(u_2+D_1+bu_3)^2}, y_{31} = du_3$,
$$y_{32} = \frac{-w_3u_3}{(u_2 + D_1 + bu_3)} - \frac{bw_3u_2u_3}{(u_2 + D_1 + bu_3)^2}$$
$y_{33} = -c + du_1 - \frac{w_3u_2}{(u_2+D_1+bu_3)} - \frac{bw_3u_2u_3}{(u_2+D_1+bu_3)^2}$.
The characteristic equation is as showing:

$$\lambda^3 + A\lambda^2 + B\lambda + C = 0 \tag{7}$$

where, $A = -(y_{11} + y_{22} + y_{33})$
$B = y_{11}y_{22} - y_{12}y_{21} - y_{23}y_{32}$
$C = y_{11}(y_{22}y_{33} - y_{23}y_{32}) - y_{12}y_{21}y_{33}$
Hence, E_4 is LAS, as following conditions hold: (i) A, B and $C > 0$ (ii) $AB > C$.

Global Stability Analysis
Theorem 6

If we consider that

$$\tau - \frac{wu_2}{u_1 + D} + \frac{wu_1u_2}{(u_1 + D)^2} > 0 \quad (8)$$

$$-a + \frac{wu_1}{u_1 + D} - \frac{w_2u_2u_3}{(u_2 + D_1 + bu_3)^2} + \frac{w_2u_3}{(u_2 + D_1 + bu_3)} > 0$$

$$-c + du_1 - \frac{w_3u_2}{(u_2 + D_1 + bu_3)} - \frac{bw_3u_2u_3}{(u_2 + D_1 + bu_3)^2} > 0$$

$$\left[\tau - \frac{wu_2}{u_1 + D} + \frac{wu_1u_2}{(u_1 + D)^2}\right]\left[-a + \frac{wu_1}{u_1 + D} - \frac{w_2u_2u}{(u_2 + D_1 +}\left[-a + \frac{wu_1}{u_1 + D} - \frac{w_2u_2u_3}{(u_2 + D_1 + bu_3)^2}\right.\right.$$
$$\left.+ \frac{w_2u_3}{(u_2 + D_1 + bu_3)}\right]\left[-c + du_1 - \frac{w_3u_2}{(u_2 + D_1 + bu_3)} - \frac{bw_3u_2u_3}{(u_2 + D_1 + bu_3)^2}\right]$$
$$> \frac{w_2u_2}{(u_2 + D_1 + bu_3)} - \frac{bw_2u_2u_3}{(u_2 + D_1 + bu_3)^2}$$

then $E_4 = (\tilde{u_1}, \tilde{u_2}, \tilde{u_3})$ is GAS.
Proof: Characterize a Lyapunov function

$$V = \left(u_1 - \tilde{u_1} - \tilde{u_1}\ln\frac{\tilde{u_1}}{\tilde{u_1}}\right) + \left(u_2 - \tilde{u_2} - \tilde{u_2}\ln\frac{\tilde{u_2}}{\tilde{u_2}}\right) + \left(u_3 - \tilde{u_3} - \tilde{u_3}\ln\frac{\tilde{u_3}}{\tilde{u_3}}\right)$$

Taking we differentiate w.r.t. t along the system solution, we get $\frac{dV}{dt} = -c_{11}(u_1 - \tilde{u_1})^2 - c_{22}(u_2 - \tilde{u_2})^2 - c_{33}(u_3 - \tilde{u_3})^2 + c_{12}(u_1 - \tilde{u_1})(\tilde{u_2} - \tilde{u_2}) + c_{23}(u_2 - \tilde{u_2})(u_3 - \tilde{u_3})$.

Where, $c_{11} = \tau - \frac{wu_2}{u_1+D} + \frac{wu_1u_2}{(u_1+D)^2}, c_{12} = \frac{wu_1}{(u_1+D)}, c_{13} = -fu_1, c_{21} = \frac{wu_2}{u_1+D} - \frac{w_1u_1u_2}{(u_1+D)^2}$,
$c_{22} = -a + \frac{wu_1}{u_1+D} - \frac{w_2u_2u_3}{(u_2+D_1+bu_3)^2} + \frac{w_2u_3}{(u_2+D_1+bu_3)}$, $c_{23} = \frac{w_2u_2}{(u_2+D_1+bu_3)} - \frac{bw_2u_2u_3}{(u_2+D_1+bu_3)^2}, c_{31} = du_3$,
$c_{32} = \frac{-w_3u_3}{(u_2+D_1+bu_3)} - \frac{bw_3u_2u_3}{(u_2+D_1+bu_3)^2}$
$c_{33} = -c + du_1 - \frac{w_3u_2}{(u_2+D_1+bu_3)} - \frac{bw_3u_2u_3}{(u_2+D_1+bu_3)^2}$.
if the following inequalities hold:

$$c_{11} > 0, c_{22} > 0, c_{33} > 0 \quad (11)$$
$$c_{12}^2 < c_{11}c_{22} \quad (12)$$
$$c_{23}^2 < c_{22}c_{33} \quad (13)$$

It is easy to see that all the conditions are satisfied. Biologically, the boundedness and stability of a system show that the model system is well mannered. Furthermore, it implies that no species grows exponentially for a long period.

Attack Rate of Generalist Predator on Specialist Predator ω_2

The attack rate of a generalist predator is indeed a crucial parameter in predator-prey models, influencing the dynamics, stability, and equilibrium states of the system. By examining how the attack rate affects these aspects, ecologists can better understand and predict the impacts of changes in predator efficiency or environmental conditions on population dynamics. Numerically, the system stabilizes when $\omega_2 = 1.78$ as shown in figure 2 and stays constant until it reaches$\omega_2 = 5$. Moreover, when$\omega_2 = 6.78$, the system becomes unstable.

Hopf-bifurcation of Non-spatial System

Here, we have established a theorem that clarifies Hopf bifurcation, where k_1 stands for the bifurcation parameter.

Theorem 7

Hopf-bifurcation occurs in model system (1)-(3), When carrying capacityk_1, crosses a threshold valuek_1', near $E_4 = (\tilde{u}, \tilde{v}, \tilde{w})$ if conditions hold as: $A(k_1) > 0, C(k_1) > 0, A(k_1')B(k_1') - C(k_1') = 0$ and$[A(k_1')B(k_1')]' \neq C'(k_1')$.

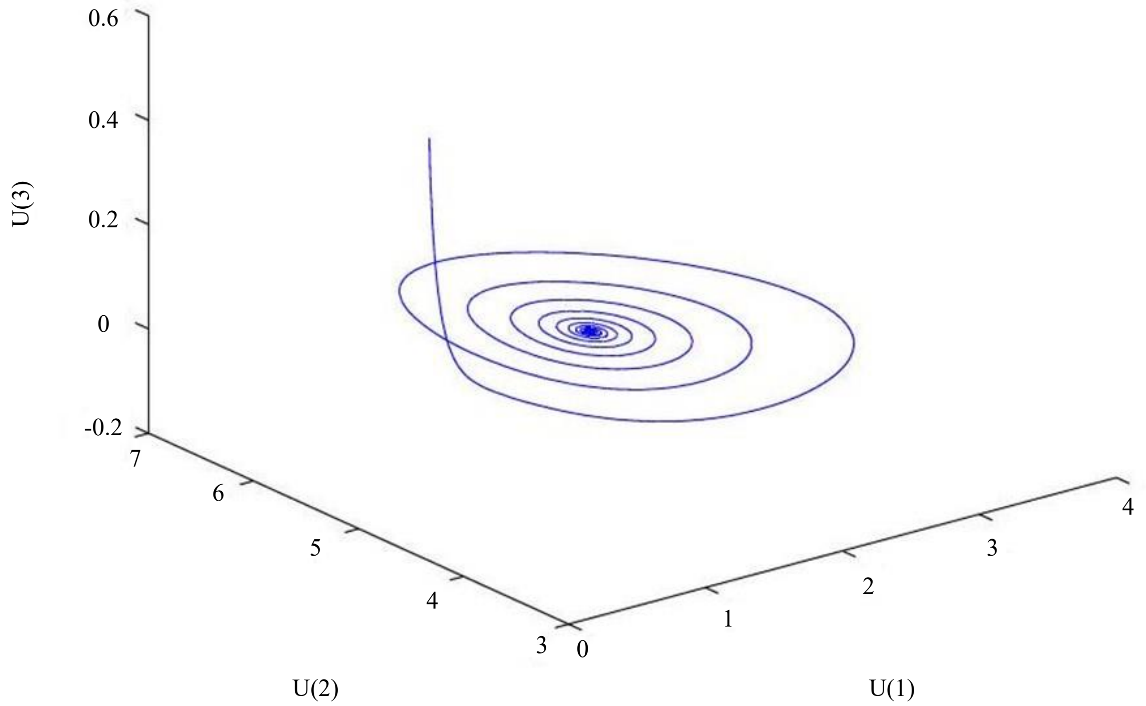

Figure 2. Effect of attack rate $\boldsymbol{\omega_2 = 1.78}$.

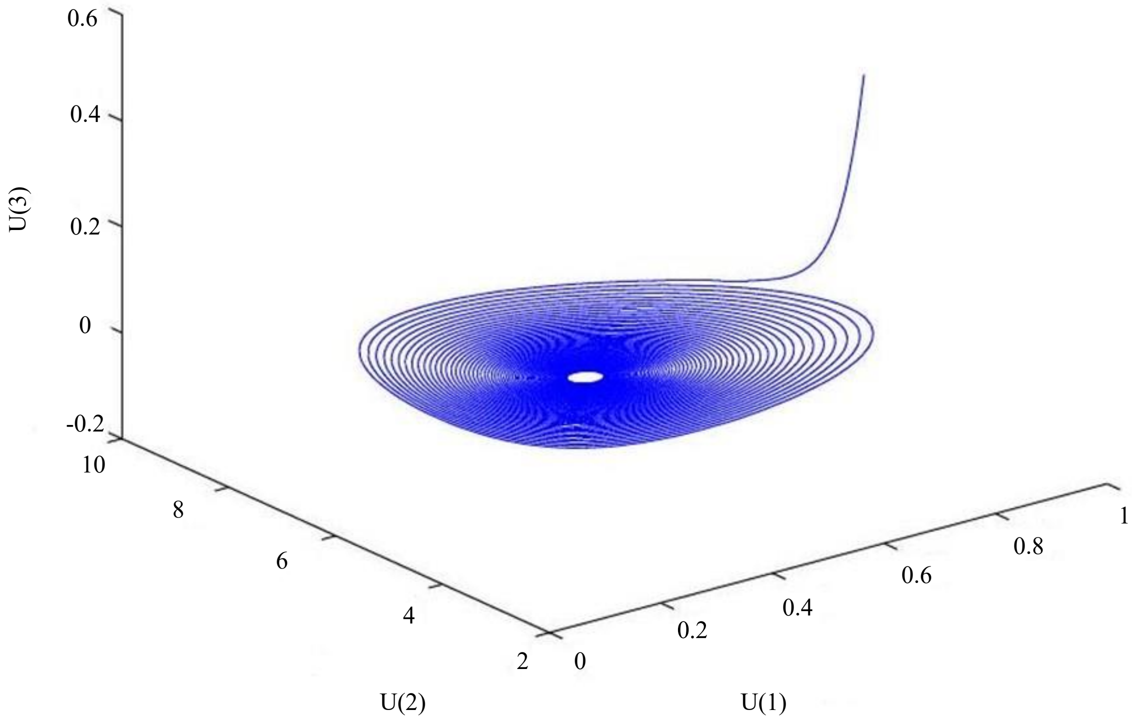

Figure 3. Effect of attack rate $\boldsymbol{\omega_2 = 6.78}$.

Proof: It is easy to see that $\boldsymbol{E_4}$ is LAS. If threshold value $\boldsymbol{k_1'}$ exist s.t. $\boldsymbol{A(k_1')B(k_1') - C(k_1') = 0}$ For $\boldsymbol{k_1 = k_1'}$ the characteristic equation is as:

$$\boldsymbol{\left(\lambda^2(k_1') + B(k_1')\right)\left(\lambda(k_1') + A(k_1')\right) = 0}$$

Roots are: $-A(k_1'), \iota\sqrt{B(k_1')}$ and $-\iota\sqrt{B(k_1')}$. If transversality condition $\left.\frac{\mathbf{Re}(\lambda(B))}{dk_1}\right|_{k_1=k_1'} \neq \mathbf{0}$ hold, then Hopf-bifurcation occurs at $k_1 = k_1'$. roots are $\lambda_1(k_1) = \mu(k_1) + \iota\nu(k_1)$, $\lambda_2(k_1) = \mu(k_1) + \iota\nu(k_1)$, $\lambda_3(k_1) = -A(k_1)$.

Substituting into we get
$Q(k_1)\mu'(k_1) - L(k_1)\nu'(k_1) + M(k_1) = 0$,
$L(k_1)\mu'(k_1) + Q(k_1)\nu'(k_1) + N(k_1) = 0$,
Where,
$Q(k_1) = 3u^2(k_1) + 2A(k_1)\mu(k_1) + B(k_1) - 3\nu^2(k_1)$
$L(k_1) = 6\mu(k_1)\nu(k_1) + 2A\nu(k_1)$
$M(k_1) = \mu^2(k_1)A'(k_1) + k_1'\mu(k_1) + C'(k_1) - A'(k_1)\nu^2(k_1)$
$N(k_1) = 2\mu(k_1)\nu(k_1)A'(k_1) + B'(k_1)\nu(k_1)$.
Here, $\mu(k_1) = 0, \nu(k_1) = \sqrt{B(k_1')}$, we get $Q(k_1') = -2B(k_1'), L(k_1') = 2A(k_1')\sqrt{B(c')}$, $M(k_1') = C'(k_1') - A'(k_1')B(k_1')$, $N(k_1') = B'(k_1')\sqrt{B(k_1')}$.

Solving $\mu'(k_1)$, we get:

$$\left.\frac{\mathbf{Re}(\lambda_j(k_1))}{dk_1}\right|_{k_1=k_1'} = \mu'(k_1)_{k_1=k_1'} = -\frac{L(k_1')N(k_1') + Q(k_1')M(k_1')}{Q^2(k_1') + L^2(k_1')} = \frac{1}{2}$$

$\frac{C'(k_1') - \left(A(k_1')B(k_1')\right)'}{A^2(k_1') + B(k_1')} \neq 0$. If $\left(A(k_1')B(k_1')\right)' \neq C'(k_1')$ and $\lambda_3(k_1') = -A(k_1') < 0$.
Hence the theorem is proved.

Center Manifold Theorem

Center Manifold theorem is applied to check stability if one or more roots are zero and next one is negative real part. Now we shift $E(u^1, u^2, u^3)$ at the origin and get the transformation $u_1 = u_1' + u^1, u_2 = u_2' + u^2, u_3 = u_3' + u^3$ in the system (4)-(6) and we get (omitting the dash sign and neglecting the third and higher order terms)

$$\frac{du_1}{dt} = x_{11}u_1 + x_{12}u_2 + x_{13}u_3 + x_{14}u_1^2 + x_{15}u_1u_2 + x_{16}u_1^2 + x_{17}u_2u_3 + x_{18}u_3^2 + x_{19}u_1u_3$$
$$\frac{du_2}{dt} = x_{21}u_1 + x_{22}u_2 + x_{23}u_3 + x_{24}u_1^2 + x_{25}u_1u_2 + x_{26}u_2^2 + x_{27}u_2u_3 + x_{28}u_3^2 + x_{29}u_1u_3$$
$$\frac{du_3}{dt} = x_{31}u_1 + x_{32}u_2 + x_{33}u_3 + x_{34}u_1^2 + x_{35}u_1u_2 + x_{36}u_2^2 + x_{37}u_1u_3 + x_{38}u_3^2 + x_{39}u_1u_3$$

Here, the coefficients x_{ij} are given in Appendix A. System turns as:

$$\begin{bmatrix}\dot{u_1}\\ \dot{u_2}\\ \dot{u_3}\end{bmatrix} = \begin{bmatrix}x_{11} & x_{12} & x_{13}\\ x_{21} & x_{22} & x_{23}\\ x_{31} & x_{32} & x_{33}\end{bmatrix}\begin{bmatrix}u_1\\ u_2\\ u_3\end{bmatrix} + \begin{bmatrix}x_{14}u_1^2 + x_{15}u_1u_2 + x_{19}u_1u_3\\ x_{24}u_1^2 + x_{25}u_1u_2 + x_{27}u_1u_3\\ x_{37}u_2u_3 + x_{39}u_1u_3\end{bmatrix}$$

Theorem 8

Eigen values of $J(E_1)$ is a saddle point. Proof: For E_1 the above system reduce to,

$$\begin{bmatrix}\dot{u_1}\\ \dot{u_2}\\ \dot{u_3}\end{bmatrix} = \begin{bmatrix}-\tau & \frac{w}{k_1 + D} & -fk_1\\ 0 & -a + \frac{wk_1}{k_1 + D} & 0\\ 0 & 0 & -c + dk_1\end{bmatrix}\begin{bmatrix}u_1\\ u_2\\ u_3\end{bmatrix} + \begin{bmatrix}x_{14}u_1^2 + x_{15}u_1u_2 + x_{19}u_1u_3\\ x_{24}u_1^2 + x_{25}u_1u_2 + x_{27}u_1u_3\\ x_{37}u_2u_3 + x_{39}u_1u_3\end{bmatrix}$$

E.V. is given as $-\boldsymbol{\tau}, -\boldsymbol{a}+\frac{\boldsymbol{wk_1}}{\boldsymbol{k_1+D}}$ and $-\boldsymbol{c}+\boldsymbol{dk_1}$. If we consider $\boldsymbol{a}=\frac{\boldsymbol{wk_1}}{\boldsymbol{k_1+D}}$ then the equilibrium point $\boldsymbol{E_1(k_1,0,0)}$ is non-hyperbolic type. Now we use the transformation

$$\begin{bmatrix}\boldsymbol{u_1}\\ \boldsymbol{u_2}\\ \boldsymbol{u_3}\end{bmatrix}$$

Then the system turns as,

$$\begin{bmatrix}\dot{x}\\ \dot{y}\\ \dot{z}\end{bmatrix}=\begin{bmatrix}-\tau & 0 & 0\\ 0 & 0 & 0\\ 0 & 0 & -c+dk_1\end{bmatrix}\begin{bmatrix}x\\ y\\ z\end{bmatrix}+\begin{bmatrix}H_1\\ H_2\\ H_3\end{bmatrix}$$

We can see $\boldsymbol{H_i}$ in Appendix B. Now $\boldsymbol{W^c(0)=(x,y,z)\epsilon R^3: x=g_1(y), z= g_2(y), g_1(0)=0, g_2(0)=0, Dg_1(0)= 0, Dg_2(0)=0}$, To calculate $\boldsymbol{W^c(0)}$, let us consider $\boldsymbol{x=g_1(y)=c_{11}y^2+c_{12}y^3+O(\|y\|^4)}$,
$\boldsymbol{z=g_2(y)=c_{21}y^2+c_{22}y^3+O(\|y\|^4)}$. Now we find $\boldsymbol{c_{11}=0, c_{12}=N_{13}, c_{21}=0, c_{22}=0}$. Thus, manifold is shown by $\boldsymbol{\dot{y}=N_{22}y^2+N_{21}N_{13}y^4}$, it is a saddle point. Hence proved.

Theorem 9

At $\boldsymbol{E_4}$, the periodic solution will be stable and unstable if $\boldsymbol{\Lambda<0}$ and $\boldsymbol{\Lambda>0}$ respectively. Proof:If Hopf bifurcation exists in the system, it implies that characteristic equations have purely complex conjugates and one negative real root. The roots are given as $\boldsymbol{-A_1, i\sqrt{A_2}, -i\sqrt{A_2}}$. It is non-hyperbolic type roots. Therefore: $\begin{bmatrix}\boldsymbol{u_1}\\ \boldsymbol{u_2}\\ \boldsymbol{u_3}\end{bmatrix}=\mathbf{A}\begin{bmatrix}\boldsymbol{x}\\ \boldsymbol{y}\\ \boldsymbol{z}\end{bmatrix}$
Where, $\begin{bmatrix}\boldsymbol{g_{11}} & \boldsymbol{g_{12}} & \boldsymbol{g_{13}}\\ \boldsymbol{g_{21}} & \boldsymbol{g_{22}} & \boldsymbol{g_{23}}\\ \boldsymbol{g_{31}} & \boldsymbol{g_{32}} & \boldsymbol{g_{33}}\end{bmatrix}$, $\boldsymbol{g_{ij}}$ is given in Appendix C.
The system becomes:

$$\begin{bmatrix}\dot{x}\\ \dot{y}\\ \dot{z}\end{bmatrix}=\begin{bmatrix}0 & -\sqrt{A_2} & 0\\ \sqrt{A_2} & 0 & 0\\ 0 & 0 & -A_1\end{bmatrix}\begin{bmatrix}x\\ y\\ z\end{bmatrix}+\begin{bmatrix}e_1\\ e_2\\ e_3\end{bmatrix}$$

We can see AppendiX D to check the values of $\boldsymbol{e_1, e_2}$ and $\boldsymbol{e_3}$. Characteristic equations have purely complex conjugate and one negative real root. Therefore, we are unable to find stability, so the Center manifold is given as:

$\boldsymbol{W^c(0)=(x,y,z)\epsilon R^3: z=g(x,y), |x|<\delta_1, |y|< \delta_2, g(0,0)=0, Dg(0,0)=0}$. To calculate the center manifold theorem, we consider $\mathbf{z=g(x,y)} \boldsymbol{=a_1x^2+a_2y^2+a_3xy+O(\|x\|^3)}$, Here we find $\boldsymbol{a_1=\frac{1}{A_1}(A_{31}-a_3\sqrt{A_2}), a_2=\frac{1}{A_2}(A_{32}-a_3\sqrt{A_2})}$ and $\boldsymbol{a_3=\frac{A_1A_2A_{34}-2\sqrt{A_2}(A_{32}A_1-A_{31}A_2)}{(2A_1+2A_2+A_1^2)A_2}}$.
Thus, by using the center manifold:

$$\begin{bmatrix}\dot{x}\\ \dot{y}\end{bmatrix}=\begin{bmatrix}0 & -\sqrt{A_2}\\ \sqrt{A_2} & 0\end{bmatrix}\begin{bmatrix}x\\ y\end{bmatrix}+\begin{bmatrix}f_1\\ f_2\end{bmatrix}$$

Where $\boldsymbol{f_1(x,y)=A_{11}x^2+A_{12}y^2+A_{14}xy+ A_{16}a_1x^3+A_{15}a_2y^3+(A_{15}a_1+A_{16}a_3)x^2y+(A_{15}a_3+A_{16}a_2)y^2x+ O(\|X\|^4), f_2=A_{21}x^2+A_{22}y^2+A_{24}xy+A_{26}a_1x^3+ A_{25}a_2y^3+A_{25}a_2y^3+(A_{25}a_1+A_{26}a_3)x^2y+(A_{25}a_3+A_{26}a_2)y^2x+ O(\|X\|^4)}$.

Now, we calculate the First Lyapunov exponent $\boldsymbol{\Lambda}$ at $(\mathbf{0},\mathbf{0},\mathbf{0})$, to show stability or instability of $\boldsymbol{E_4}$.

$$\boldsymbol{\Lambda} = \frac{1}{16}\left(f_{1(xxx)} + f_{1(yyy)} + f_{2(xxx)} + f_{2(yyy)}\right) + \frac{1}{16\sqrt{A_2}}\left[f_{1(xy)}\left(f_{1(xx)} + f_{1(yy)}\right) - f_{2(xy)}\left(f_{2(xx)} + f_{2(yy)}\right)\right] - f_{1(xx)}f_{2(xx)} + f_{1(yy)}f_{2(yy)}$$

$$= \frac{1}{16}\left[6A_{16}a_1 + 2(A_{15}a_3 + A_{16}a_2) + 2(A_{25}a_1 + A_{26}a_3) + 6A_{25}a_3\right] + \frac{1}{16\sqrt{A_2}}\left[2A_{14}(A_{11} + A_{12}) - 2A_{24}(A_{21} + A_{22}) - 4A_{11}A_{21} + 4A_{12}A_{22}\right]$$

Hence theorem is proved.

Numerical Simulation

Now, we will perform numerical analysis supporting the analytical findings. We used ode45 solver in MATLAB by taking the parameter values as: $\boldsymbol{\tau = 0.90, k_1 = 12, w_3 = 1.78}$, $\mathbf{f = .01}$, $\boldsymbol{D_1 = 7.2}$, $\mathbf{b = .01, a = .23, w = 2.15, D = 13.51, c = 5}$, $\mathbf{d = .01}$, $\boldsymbol{w_2 = 1.78}$.

First, we see the effect of attack rate of generalist predator on specialist predator $\boldsymbol{\omega_2}$ has been shown in Figure 2-3. The system becomes unstable at $\boldsymbol{\omega_2 = 7.78}$. When we increase the value of $\boldsymbol{\omega_2}$ system remains unstable. Secondly, we see the outcome of constant $\boldsymbol{k_1}$ as shown in Figures. 4-7. The diagrams indicate that the system become stable in figure 5 at $\boldsymbol{k_1 = 15}$, as we increase the value of $\boldsymbol{k_1}$ it tends to Hopf bifurcation at the critical value $\boldsymbol{k_1 = 16}$ in figure 6. To better understand, at different values of $\boldsymbol{k_1}$, we observe some of time series and phase portrait diagrams. Our MATLAB simulations successfully demonstrate how variations in $\boldsymbol{k_1}$ affect stability and cause bifurcation, hence validating the theoretical predictions. The numerical results offer important insights into the dynamics of ecosystems by depicting the dynamical alterations in predator-prey interactions.

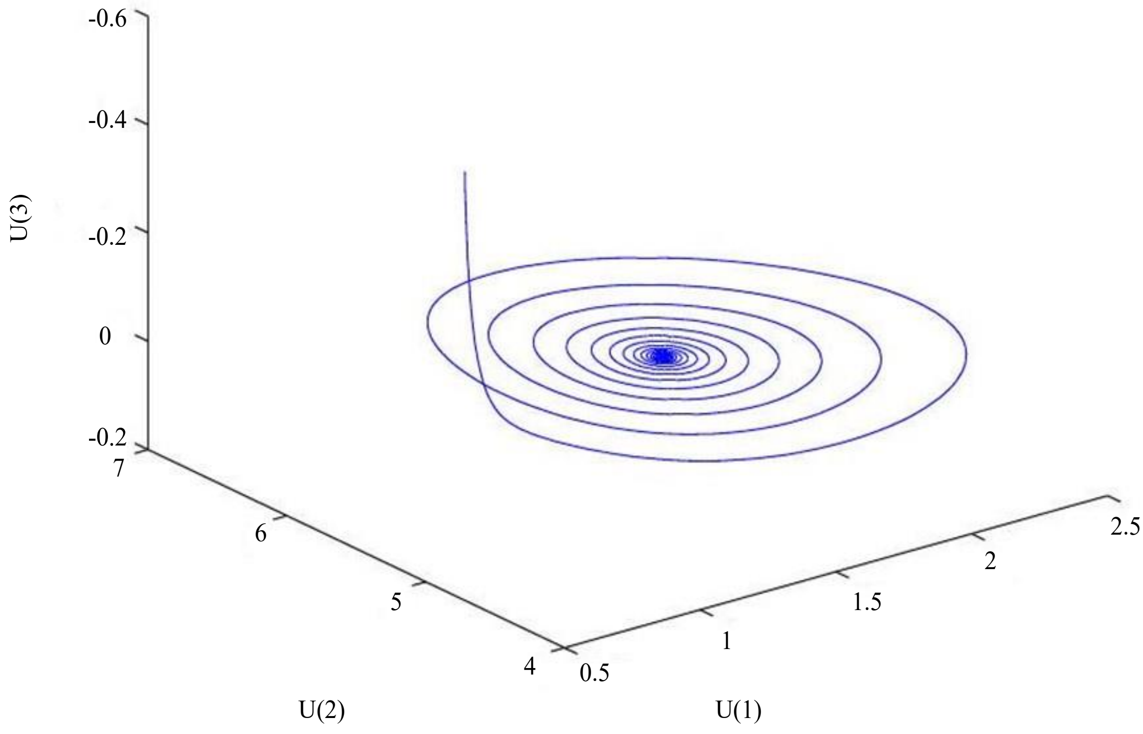

Figure 4. Existence of Hopf bifurcation at $\boldsymbol{k_1 = 12.}$

DISCUSSION AND CONCLUSION

This work investigates a three-dimensional food chain model in which Boddington-DeAngelis and Holling type-II functional responses endows the prey with refuge capabilities. It shows a major role to preserve the dynamical system balance. There is a schematic illustration is given in Figure 1 to help visualize the model formulation. The proposed system is investigated using differential equation theory and several dynamical techniques like boundedness, local stability, global stability, and bifurcation. Next, we showed that the solutions had uniform boundaries. We determined equilibrium points and examined their stability. Effect of attack rate of generalist predator on specialist predator $\boldsymbol{\omega_2}$ has been shown in Figure 2-3. The system becomes unstable at$\boldsymbol{\omega_2 = 7.78}$. When we increase the value of $\boldsymbol{\omega_2}$ system remains unstable. We conclude that attack rate of a generalist predator is a crucial parameter in predator-prey models, influencing the dynamics, stability and equilibrium states of the system. By modifying the attack rate, ecologists can predict how changes in predator efficiency or environmental conditions might impact population dynamics. We have also observed that inhibitory effects are essential for dynamical system's stability and control. Inhibitory mechanisms work to keep the system in equilibrium by adjusting the activity of its constituent parts. Moreover, we found a Hopf bifurcation see in Figure 4-7 with parameter$\boldsymbol{k_1}$. As the value of $\boldsymbol{k_1}$ become larger system become unstable. Bifurcation diagrams display the model system's incredibly intricate and rich dynamical behavior. Also, these diagrams show the significant importance of the model and related to real-life systems. For advancement, we have given the numerical solutions using MATLAB to validate analytical results for temporal model system.

Refuge ability refers to the capacity of prey to find access and effectively use these safe zones to avoid predators. Numerous elements, including the prey's movement, sensory perception, and behavioral adaptations, can affect this capacity. The study examines these factors and their impact on the prey's survival rates in the presence of predators. We have used the Beddington-DeAngelis and Holling type II functional responses to study the dynamics of the prey predator system in order to understand the protective character of prey. Finally, we wind up that the model become real when we consider features like Beddington-DeAngelis and Holling type II functional responses. It increases the value of the work. By combining Beddington-DeAngelis and Holling Type II functional responses a combination that hasn't been investigated before this study offers a fresh and thorough viewpoint on ecological modeling. With possible uses in ecological conservation and population management tactics, the findings advance our knowledge of stability mechanisms, bifurcation behavior, and predator-prey interactions.

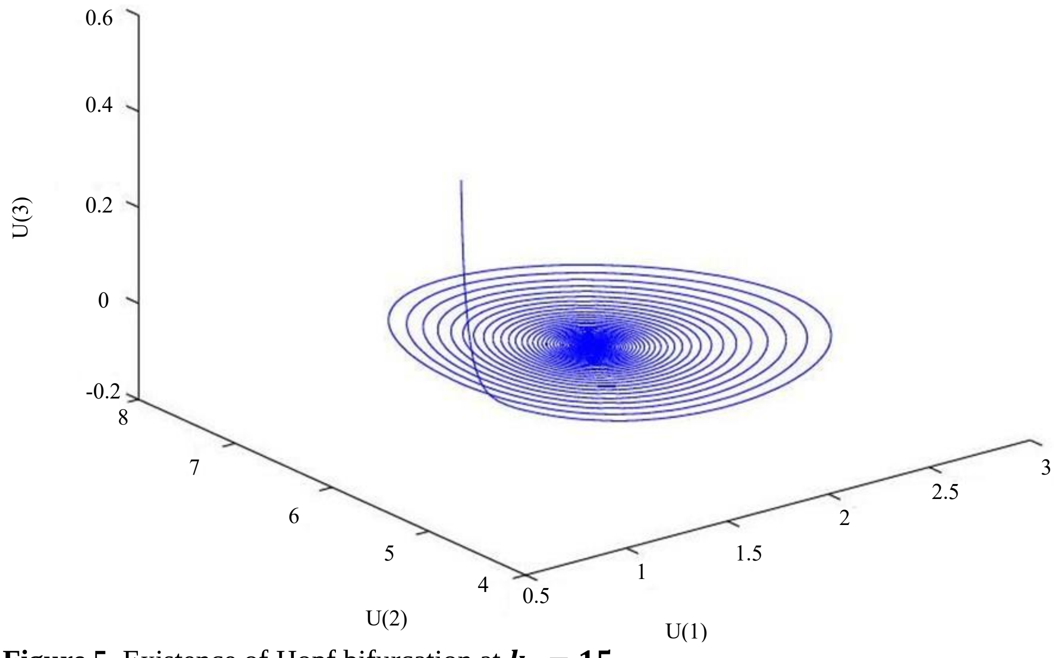

Figure 5. Existence of Hopf bifurcation at $\boldsymbol{k_1 = 15}$.

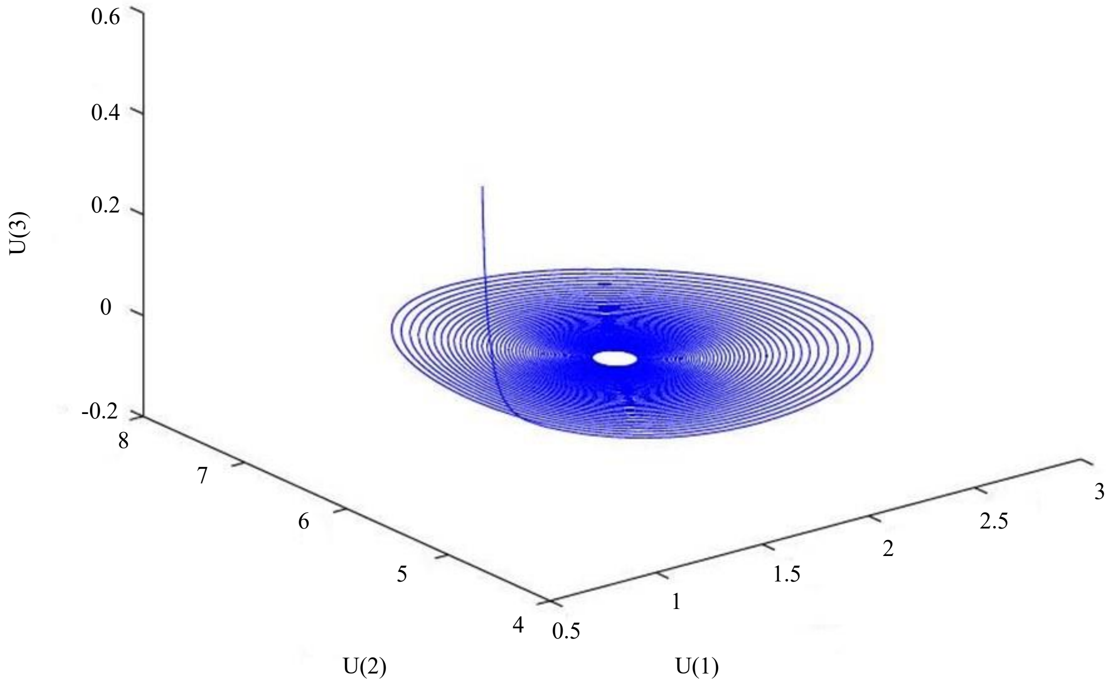

Figure 6. Existence of Hopf bifurcation at $k_1 = 16$.

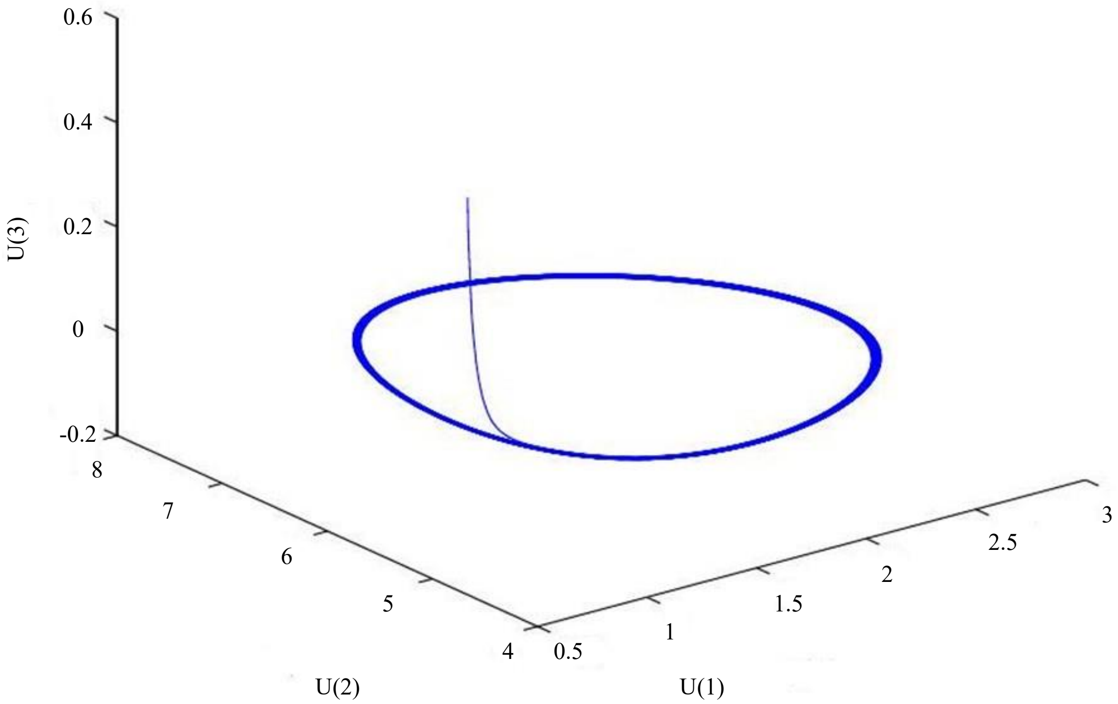

Figure 7. Existence of Hopf bifurcation at $k_1 = 17$.

It shows originality of this article which is be used in different real-life ecological systems. Disclosure of conflicting interests. The authors declare that none of the work provided in this study appears to have been influenced by any known conflicts of interest, either financial or personal.

APPENDICES

Appendix A

$x_{11} = \tau - \frac{wu_2}{u_1+D} + \frac{wu_1u_2}{(u_1+D)^2}, x_{12} = \frac{wu_1}{(u_1+D)},$

Journal of Polymer & Composites
Volume 13, Special Issue 3
ISSN: 2321-2810 (Online), ISSN: 2321-8525 (Print)

$x_{13} = -fu_1, x_{21} = \frac{wu_2}{u_1+D} - \frac{w_1u_1u_2}{(u_1+D)^2},$
$x_{22} = -a + \frac{wu_1}{u_1+D} - \frac{w_2u_2u_3}{(u_2+D_1+bu_3)^2} + \frac{w_2u_3}{(u_2+D_1+bu_3)},$
$x_{23} = \frac{w_2u_2}{(u_2+D_1+bu_3)} - \frac{bw_2u_2u_3}{(u_2+D_1+bu_3)^2}, x_{31} = du_3,$
$x_{32} = \frac{-w_3u_3}{(u_2 + D_1 + bu_3)} - \frac{bw_3u_2u_3}{(u_2 + D_1 + bu_3)^2}$
$x_{33} = -c + du_1 - \frac{w_3u_2}{(u_2 + D_1 + bu_3)} - \frac{bw_3u_2u_3}{(u_2 + D_1 + bu_3)^2}$
$x_{14} = \frac{2wu_2}{(u_1 + D)^2} - \frac{2wu_1u_2}{(u_1 + D)^3}$
$x_{15} = \frac{-wu_1}{(u_1 + D)^2} + \frac{w}{(u_1 + D)}$
$x_{16} = -f$
$x_{17} = 0$
$x_{18} = 0$
$x_{19} = 0$
$x_{24} = \frac{wu_2}{(u_1 + D)^2} - \frac{wu_2}{(u_1 + D)^2} + \frac{2wu_1u_2}{(u_1 + D)^3}$
$x_{25} = \frac{w}{(u_1 + D) - \frac{-w_1u_1}{(u_1 + D)^2}}$
$x_{26} = 0$
$x_{27} = \frac{-wu_2b}{(u_2 + D_1 + bu_3)^2} + \frac{bw_2w_3}{(u_2 + D_1 + bu_3)} - \frac{b^2u_2u_3w_2}{(u_2 + D_1 + bu_3)^2}$
$x_{28} = \frac{w_2u_3}{(u_2 + D_1 + bu_3)^2} - \frac{w_2u_2u_3b}{(u_2 + D_1 + bu_3)^3} + \frac{w_2u_2b}{(u_2 + D_1 + bu_3)} -$
$\frac{w_2u_3b}{(u_2 + D_1 + bu_3)^2}$
$x_{29} = 0$
$x_{34} = 0$
$x_{35} = 0$
$x_{36} = 0$
$x_{37} = d$
$x_{38} = \frac{w_3u_3}{(u_2 + D_1 + bu_3)^2} - \frac{w_3u_3b}{(u_2 + D_1 + bu_3)^2} + \frac{w_3u_2u_3b}{(u_2 + D_1 + bu_3)^3}\ x_{39} = d$

6.2 Appendix B

The values of H_i is as follows: $H_1 = x^2 + N_{11}xy + M_{12}xz + M_{13}y^2 + M_{14}yz + M_{15}z^2, H_2 = M_{21}xy + M_{22}v^2 + M_{23}yz, H_3 = M_{31}xz + M_{32}yz + M_{33}z^2$.

6.3 Appendix C

Here, $g_{11} = -A_2, g_{12} = 0, g_{13} = A_1^2 - x_{23}x_{32}, g_{21} = x_{31}x_{23}, g_{22} = -x_{21}\sqrt{A_2}, g_{23} = x_{31}x_{23} - x_{21}A_1, g_{31} = 0, g_{32} = -x_{31}\sqrt{A_2}, g_{23} = x_{21}x_{32} - x_{31}A_1$

6.4 Appendix D

$$e_1 = D_{11}x^2 + D_{12}y^2 + D_{13}z^2 + D_{14}xy + D_{15}yz + D_{16}zx$$
$$e_2 = D_{21}x^2 + D_{22}y^2 + D_{23}z^2 + D_{24}xy + D_{25}yz + D_{26}zx$$
$$e_3 = D_{31}x^2 + D_{32}y^2 + D_{33}z^2 + D_{34}xy + D_{35}yz + D_{36}zx$$

with, $D_{11} = C_{11}g_{11}^2 + A_{12}g_{11}g_{21}$,
$D_{12} = C_{14}g_{22}g_{32}$,

$\boldsymbol{D_{13} = C_{11}g_{13}^2 + C_{12}g_{13}g_{23} + C_{13}g_{13}g_{33} + C_{14}g_{23}g_{33}}$,
$\boldsymbol{D_{14} = C_{12}g_{11}g_{22} + C_{13}g_{11}g_{32} + C_{14}g_{21}g_{32}}$
$\boldsymbol{D_{15} = C_{11}g_{13}g_{22} + C_{13}g_{13}g_{32} + C_{14}g_{22}g_{33} + C_{14}g_{23}g_{32}}$,

$$\boldsymbol{D_{16} = 2C_{11}g_{11}g_{13} + C_{12}g_{11}g_{23} + C_{12}g_{13}g_{21} + C_{13}g_{11}g_{33} + C_{14}g_{21}g_{33}}$$

The similar expression for $\boldsymbol{D_{2i}}$ and $\boldsymbol{D_{3i}}$ will be obtained only replacing $\boldsymbol{C_{1j}}$ by $\boldsymbol{C_{2j}}$ and $\boldsymbol{C_{3j}}$ respectively.

$\boldsymbol{C_{11} = t_{11}x_{14} + t_{12}x_{24}}$
$\boldsymbol{C_{12} = t_{11}x_{15} + t_{12}x_{25}}$
$\boldsymbol{C_{13} = t_{11}x_{19} + t_{13}x_{39}}$
$\boldsymbol{C_{14} = t_{12}x_{27} + t_{13}x_{39}}$
$\boldsymbol{C_{21} = t_{21}x_{14} + t_{22}x_{24}}$
$\boldsymbol{C_{22} = t_{21}x_{15} + t_{22}x_{25}}$
$\boldsymbol{C_{23} = t_{21}x_{19} + t_{23}x_{39}}$
$\boldsymbol{C_{24} = t_{22}x_{27} + t_{23}x_{39}}$
$\boldsymbol{C_{31} = t_{11}x_{14} + t_{12}x_{24}}$
$\boldsymbol{C_{32} = t_{31}x_{15} + t_{32}x_{25}}$
$\boldsymbol{C_{33} = t_{31}x_{19} + t_{33}x_{39}}$
$\boldsymbol{C_{34} = t_{32}x_{27} + t_{33}x_{39}}$

Where,

$$\boldsymbol{A^{-1} = \begin{bmatrix} t_{11} & t_{12} & t_{13} \\ t_{21} & t_{22} & t_{23} \\ t_{31} & t_{32} & t_{33} \end{bmatrix}}$$

with $\boldsymbol{t_{11}} = \frac{g_{22}g_{33}-g_{23}g_{32}}{|A|}, \boldsymbol{t_{12}} = \frac{g_{32}g_{13}}{|A|}, \boldsymbol{t_{13}} = \frac{-g_{13}g_{22}}{|A|}, \boldsymbol{t_{21}} = \frac{-g_{21}g_{33}}{|A|}, \boldsymbol{t_{22}} = \frac{g_{11}g_{33}}{|A|}, t_{23} = \frac{g_{13}g_{21}-g_{11}g_{23}}{|A|}, t_{31} = \frac{g_{21}g_{32}}{|A|}, t_{32} = \frac{-g_{11}g_{32}}{|A|}, t_{33} = \frac{g_{11}g_{22}}{|A|}$ where, $|A|$ represents the determinant of A .

REFERENCES

1. Baghel RS, Dhar J. Pattern formation in three species food web model in spatiotemporal domain with Beddington-DeAngelis functional response. *Nonlinear Anal Model Control*. 2014;19(2):155–71.
2. Baghel RS, Dhar J, Jain R. Bifurcation and spatial pattern formation in spreading of disease with incubation period in a phytoplankton dynamics. *Electron J Differ Equ*. 2012;2012(21):1–12.
3. Dhar J, Baghel RS. Role of dissolved oxygen on the plankton dynamics in spatiotemporal domain. *Model Earth Syst Environ*. 2016;2(1):6.
4. Ma Z, Wang S, Wang T, Tang H. Stability analysis of prey-predator system with Holling type functional response and prey refuge. *Adv Differ Equ*. 2017;2017:1–12.
5. Jabr EAA-H, Bahlool DK. The dynamics of a food web system: Role of a prey refuge depending on both species. *Iraqi J Sci*. 2021;639–57.
6. Jawad S, Naji RK. The influence of stage structure and prey refuge on the stability of the predator-prey model. *Int J Eng Manuf*. 2022;3:51–9.
7. Kar TK. Modelling and analysis of a harvested prey-predator system incorporating a prey refuge. *J Comput Appl Math*. 2006;185(1):19–33.
8. Holt RD. Food webs in space: On the interplay of dynamic instability and spatial processes. *Ecol Res*. 2002; 17:261–73.
9. Nath B, Kumari N, Kumar V, Das KP. Refugia and Allee effect in prey species stabilize chaos in a tri-trophic food chain model. Differ Equ Dyn Syst. 2019;1–27
10. Kumar V, Kumari N. Bifurcation study and pattern formation analysis of a tri-trophic food chain model with group defense and Ivlev-like nonmonotonic functional response. Chaos Solitons Fractals. 2021; 147:110964.
11. Upadhyay RK, Banerjee M, Parshad R, Raw SN. Deterministic chaos versus stochastic oscillation in a prey-predator-top predator model. Math Model Anal. 2011;16(3):343–64.
12. Upadhyay RK, Thakur NK, Rai V. Diffusion-driven instabilities and spatiotemporal patter aquatic predator-prey system with Beddington-DeAngelis type functional response. Int JBifurcation Chaos. 2011;21(3):663–84.

13. Thakur NK. Turing and non-Turing patterns in diffusive plankton model. Comput Ecol Softw. 2015;5(1):16.
14. Upadhyay RK, Naji RK. Dynamics of a three-species food chain model with Crowley-Martin type functional response. Chaos Solitons Fractals. 2009;42(3):1337–46.
15. Zhao M, Lv S. Chaos in a three-species food chain model with a Beddington-DeAngelis functional response. Chaos Solitons Fractals. 2009;40(5):2305–16.
16. Upadhyay RK, Thakur NK, Dubey B. Nonlinear non-equilibrium pattern formation in a spatial
a. aquatic system: Effect of fish predation. J Biol Syst. 2010;18(1):129–59.
17. Baghel RS. Dynamical behaviour changes in response to various functional responses: Temporal and spatial plankton system. Iran J Sci. 2023;47(2):445–55.
18. Baghel RS, Dhar J, Jain R. Analysis of a spatiotemporal phytoplankton dynamics: Higher order stability and pattern formation. World Acad Sci Eng Technol. 2011; 60:1406–12.
19. Kumari S, Upadhyay RK. Dynamics comparison between non-spatial and spatial system of the plankton-fish interaction model. Nonlinear Dyn. 2020;99(3):2479–50.
20. Baghel RS. Spatiotemporal dynamics of toxin-producing phytoplankton–zooplankton interactions with Holling Type II functional responses. Results Control Optim. 2024; 17:100478.
21. Callahan TK, Knobloch E. Pattern formation in three-dimensional reaction-diffusion systems. Physica D Nonlinear Phenom. 1999;132(3):339–62.
22. Rai V, Upadhyay RK. Chaotic population dynamics and biology of the top-predator. Chaos Solitons Fractals. 2004;21(5):1195–204.
23. Baghel RS, Dhar J, Jain R. Bifurcation and spatial pattern formation in spreading of disease with incubation period in a phytoplankton dynamic. Electron J Differ Equ. 2012;2012(21):1–12.
24. Baghel RS, Dhar J, Jain R. Higher order stability analysis of a spatial phytoplankton dynamics: bifurcation, chaos, and pattern formation. Int J Math Model Simul Appl. 2012; 5:113–27.
25. Odhiambo F, Aminer T, Okelo B, Manyala J. Dynamical analysis of prey refuge effects on the stability of Holling Type III four-species predator-prey system. Results Control Optim. 2024;100390.
26. Maionchi DO, Reis SFD, Aguiar MAMD. Chaos and pattern formation in a spatial tri-trophic food chain. Ecol Model. 2006;191(2):291–303.
27. Baghel RS, Pareek S. Influence of nanoparticles on the spatiotemporal dynamics of phytoplankton–zooplankton interaction system. Int J Biomathematics. 2024;2450131.
28. Baghel RS, Pareek S. A complex dynamical study of spatiotemporal plankton-fish interaction with effects of harvesting. Iran J Sci. 2024;48(2):409–21.
29. Agarwal K, Baghel RS, Parmar A, et al. Jeffery Slip fluid flow with the magnetic dipole effect over a melting or permeable linearly stretching sheet. Int J Appl Comput Math. 2024; 10:5.

